AD

ORIENTATED NANO-COMPOSITES: RELATIONSHIPS BETWEEN NANO-STRUCTURE AND MECHANICAL PROPERTIES

FINAL TECHNICAL REPORT

BY

A.J. KINLOCH & A.C. TAYLOR

NOVEMBER 2004

UNITED STATES ARMY

EUROPEAN RESEARCH OFFICE OF THE U.S. ARMY

LONDON, ENGLAND

CONTRACT NUMBER N62558-03-M-0048

IMPERIAL COLLEGE LONDON, UK

Report Documentation Page

Form Approved
OMB No. 0704-0188

1. REPORT DATE	2. REPORT TYPE	3. DATES COVERED
2004	**N/A**	**-**

4. TITLE AND SUBTITLE	5a. CONTRACT NUMBER
Orientated Nano-Composites: Relationships Between Nano-Structure And Mechanical Properties	5b. GRANT NUMBER
	5c. PROGRAM ELEMENT NUMBER
6. AUTHOR(S)	5d. PROJECT NUMBER
	5e. TASK NUMBER
	5f. WORK UNIT NUMBER
7. PERFORMING ORGANIZATION NAME(S) AND ADDRESS(ES) **Imperial College London, UK**	8. PERFORMING ORGANIZATION REPORT NUMBER
9. SPONSORING/MONITORING AGENCY NAME(S) AND ADDRESS(ES)	10. SPONSOR/MONITOR'S ACRONYM(S)
	11. SPONSOR/MONITOR'S REPORT NUMBER(S)

12. DISTRIBUTION/AVAILABILITY STATEMENT
Approved for public release, distribution unlimited

13. SUPPLEMENTARY NOTES
The original document contains color images.

14. ABSTRACT

Epoxy nano-composites have been manufactured using a range of modifiers, including organoclays, silica nanoparticles and carbon nanotubes. The mechanical and fracture properties of these materials have been investigated, and the structure/property relationships discussed. Epoxy micro- and nano-composites have been manufactured using a range of layered silicate modifiers, including mica and nanoclays. The fracture toughness was increased by up to 150% with the addition of mica, but the material modified with the surface-treated clays generally showed a smaller toughening effect. In the present work, the degree of orientation of the particles was investigated using wide-angle X-ray scattering texture analysis. The platelets were found to be preferentially orientated parallel to the walls of the mould. However, fracture testing of specimens cut from orthogonal orientations showed that the fracture toughness was independent of specimen orientation. Hence, the orientation of the platelets has no effect on the fracture performance of silicate nanocomposites. The addition of nano-silica particles to the matrix of carbon fibre composites has been investigated. Both untoughened and rubber-toughened formulations were used, based upon an anhydride-cured epoxy. The addition of nano-silica leads to very significant increases in the toughness of the epoxy. The nano-SiO2 particles have an average particle diameter of 20 nm, and only a concentration of about 2% to 12% by mass of such nano-particles are needed to achieve significant improvements in the fracture performance. The toughening effect of carbon nanotubes and the effect of their orientation in adhesive joints has also been investigated. Firstly, attempts have been made to align nanotubes in-situ in an adhesive joint by applying an electric field. The fracture energy of these aligned samples was measured and compared to control samples with no nanotubes, and to a random nanotube orientation. A loading of 0.1% by mass of carbon nanotubes in epoxy was used. The measured fracture energies showed no significant effect of the addition and alignment of nanotubes at this very low loading. Secondly, carbon nanotubes were grown on a quartz substrate, and impregnated with a lowviscosity epoxy resin. Initial trials showed a potentially significant toughening effect. However, problems were encountered due to premature failure of the quartz substrate, and hence current work is using silicon substrates.

15. SUBJECT TERMS

16. SECURITY CLASSIFICATION OF:			17. LIMITATION OF ABSTRACT	18. NUMBER OF PAGES	19a. NAME OF RESPONSIBLE PERSON
a. REPORT	b. ABSTRACT	c. THIS PAGE			
unclassified	**unclassified**	**unclassified**	**SAR**	**28**	

Abstract

Epoxy nano-composites have been manufactured using a range of modifiers, including organoclays, silica nanoparticles and carbon nanotubes. The mechanical and fracture properties of these materials have been investigated, and the structure/property relationships discussed.

Epoxy micro- and nano-composites have been manufactured using a range of layered silicate modifiers, including mica and nanoclays. The fracture toughness was increased by up to 150% with the addition of mica, but the material modified with the surface-treated clays generally showed a smaller toughening effect. In the present work, the degree of orientation of the particles was investigated using wide-angle X-ray scattering texture analysis. The platelets were found to be preferentially orientated parallel to the walls of the mould. However, fracture testing of specimens cut from orthogonal orientations showed that the fracture toughness was independent of specimen orientation. Hence, the orientation of the platelets has no effect on the fracture performance of silicate nanocomposites.

The addition of nano-silica particles to the matrix of carbon fibre composites has been investigated. Both untoughened and rubber-toughened formulations were used, based upon an anhydride-cured epoxy. The addition of nano-silica leads to very significant increases in the toughness of the epoxy. The nano-SiO_2 particles have an average particle diameter of 20 nm, and only a concentration of about 2% to 12% by mass of such nano-particles are needed to achieve significant improvements in the fracture performance.

The toughening effect of carbon nanotubes and the effect of their orientation in adhesive joints has also been investigated. Firstly, attempts have been made to align nanotubes in-situ in an adhesive joint by applying an electric field. The fracture energy of these aligned samples was measured and compared to control samples with no nanotubes, and to a random nanotube orientation. A loading of 0.1% by mass of carbon nanotubes in epoxy was used. The measured fracture energies showed no significant effect of the addition and alignment of nanotubes at this very low loading.

Secondly, carbon nanotubes were grown on a quartz substrate, and impregnated with a low-viscosity epoxy resin. Initial trials showed a potentially significant toughening effect. However, problems were encountered due to premature failure of the quartz substrate, and hence current work is using silicon substrates.

Contents

1 Introduction

Polymeric adhesives can offer many advantages compared to the more traditional methods of joining such as bolting, brazing, welding, mechanical fasteners, etc. These include (1, 2) the ability to join dissimilar materials to give light-weight, but strong and stiff structures, such as honeycomb sandwich panels. Also, polymeric adhesives may be used to join thin-sheet material efficiently which, due to its low bearing strength, cannot be readily joined by other methods. Further, adhesive bonding frequently represents the most convenient and cost-effective joining technique and, indeed, the bonding operation can often be readily automated. For these reasons, adhesive bonding is widely used in many industries, for example in the automobile, truck, aerospace, railway and electronic industries. Epoxy adhesives represent the most common type of *structural* adhesive; the term *structural* meaning that the polymerised (i.e. cured or hardened) adhesive possesses a relatively high modulus and strength so that a load-bearing joint is formed.

When polymerised, epoxy adhesives are amorphous and highly-crosslinked (i.e. thermosetting) materials. This microstructure results in many useful properties for structural engineering applications, such as a high modulus and failure strength, low creep, and good performance at elevated temperatures. However, the structure of such thermosetting polymers also leads to one highly undesirable property in that they are relatively brittle materials, with a poor resistance to crack initiation and growth.

This work is a continuation of a project to understand and model the structure/property relationships of polymer nanocomposites (3, 4, 5, 6). The work to date has shown how the mechanical and fracture properties vary with the microstructure of the composite. The work presented here discusses the effects of using novel toughening approaches to increase the toughness of these brittle materials without degrading the other properties. These are firstly the use of organically-modified silicates (clays), secondly the addition of silica nanoparticles, and thirdly the use of carbon nanotubes. The ability to influence the orientation of these particles, and the effect of any orientation will be investigated.

2 Mechanical and Fracture Properties of Epoxy/Inorganic Micro- and Nano-composites

2.1 Introduction

In recent years the concept of forming hybrids using polymers and inorganic materials has received a significant amount of attention. Many of these studies have used surface-treated silicates, or organoclays, to produce layered-silicate nano-composites, e.g. (7, 8). A nano-composite is defined as a composite where one of the components has a dimension in the nanometre range. Many claims for the potential of these organic/inorganic hybrids have been made, but for some important combinations of materials little experimental data has been produced. For example, the addition of inorganic filler to a polymer matrix can greatly increase its stiffness, especially for thermoplastic materials in the rubbery region. However, thermosetting polymers have attracted far less attention, and much of the work that has been done using these materials has used elastomeric epoxies. Some studies have used rigid thermosets, though there have generally been no comparisons made between the properties of thermoset nano- and micro-composites. The earlier part of present work presented such data, and discussed how the morphology of the inorganic particles can affect the mechanical and fracture properties of the composites produced (3). This morphology is typically described as ‘particulate’, ‘intercalated’ or ‘exfoliated’, as identified by wide-angle X-ray scattering (WAXS) (9, 10). In an intercalated nano-composite, polymer chains enter the galleries and increase the measured spacing. For an exfoliated structure, the individual silicate layers (i.e. platelets) are pushed further apart, and the spacing becomes too large to measure using WAXS. For a particulate structure, the dimensions and structure of the particles essentially remain unchanged when introduced into the polymeric matrix.

In the previous work, the degree of particle orientation was unknown, and was its effect on the measured fracture toughness of the composites produced. Hence, in the present work the degree of orientation was investigated using wide-angle X-ray scattering texture analysis, and specimens were prepared to investigate whether the observed orientation of the particles affected the composite toughness.

2.2 Experimental

The epoxy used was a diglycidylether of bisphenol A/F, DGEBA/F, (AY105, Huntsman) cured using an amine hardener, polyoxypropylenediamine, (Jeffamine D230, Huntsman). A range of inorganic particles was used, as shown in Table 2.1, comprising unmodified and organically-modified silicates. Sheets of epoxy composite, 6mm thick, were produced as follows. The epoxy was poured into a beaker, the inorganic particles were added and the mixture was stirred using a spatula. The beaker was placed in a vacuum oven at 75°C, and the entrapped air was removed. The vacuum was then released, and the mixture was left in the oven for 24 hours. After this time the mixture was stirred and a stoichiometric amount of hardener added. The mixture was stirred

again and poured into a release-coated steel mould. The mould was placed in an oven, and the epoxy was cured for 3 hours at 75°C followed by 12 hours at 110°C (11). The plate of epoxy was removed after cooling and machined to produce fracture specimens according to the relevant standard (12).

In previous work several types of silicate were used (3), as shown in Table 2.1, but here only mica and Cloisite 25A were used. Note that the addition of the inorganic particles increased the viscosity of the epoxy resin, and hence there was a maximum concentration above which the viscosity of the resin was too high to be able to cast the sheets. For the Cloisite 25A modifier, a maximum of 15% by weight could be used. For the mica-modified epoxy, 30% by weight could be used. The particle size and aspect ratio were measured using laser light scattering (3), and are shown in Table 2.1.

The three-point bend fracture specimens were tested at a constant displacement rate of 1mm/min. The machined notch was sharpened by drawing a new razor blade across the notch tip prior to testing. (Note that the data produced were compared to data from specimens where a natural crack had been tapped into the specimen, and the fracture toughness, K_c, values using both techniques were found to be identical, within experimental error.) The glass transition temperatures of the samples were measured using differential scanning calorimetry (DSC), with a scan rate of 20°C/min.

Table 2.1: Silicate modifiers used in the present work, and the T_g and structure of the resulting epoxy composite.

Inorganic phase	Surface treatment	Particle diameter	Aspect ratio	T_g, °C	Structure
None	None	-	-	78	-
Mica R120	None	50 μm	15	80	Particulate
Cloisite Na^+	None	25 μm	4	81	Particulate
Cloisite 25A	2MHTL8	10 μm	4	85	Intercalated
Cloisite 30B	MT2EtOT	10 μm	4	84	Intercalated
Nanomer I30E	Octadecylamine	10 μm	4	79	Exfoliated

Notes:

Silicates are bentonite, except the mica R120.

2MHTL8: Dimethyl, hydrogenated tallow, 2-ethylhexyl quaternary ammonium.

MT2EtOT: Methyl, tallow, bis-2-hydroxyethyl, quaternary ammonium.

Particle diameter and aspect ratio measured using laser light scattering.

T_g and structure given for 10% by weight of silicate modifier.

2.3 Results

2.3.1 Introduction

The use of wide-angle X-ray scattering (WAXS) enabled the structure of the composites to be ascertained (5). These data are summarised in Table 2.1. The orientation of the particles was investigated using wide-angle X-ray scattering texture analysis. The effect of the orientation on the fracture toughness was also investigated.

2.3.2 WAXS Texture Analysis to Determine Particle Orientation

WAXS texture analysis was used to determine the extent of particle orientation in the epoxy composite plates from which the fracture test specimens are cut. The specimen is mounted in a holder such that it can be rotated in its own plane about an axis normal to the surface and about a horizontal axis (13). The diffraction angle of the X-ray beam is set to a constant value, equal to that of a strong peak in the WAXS spectrum of the particles. The plate is rotated and tilted, whilst maintaining a constant diffraction angle, and the intensity of the reflected signal is measured. These data are plotted on a pole figure, with contours to indicate the signal intensity. For a random distribution of particle orientations the signal intensity will be approximately constant across the whole of the pole figure. When the particles are orientated parallel to the plate surface then there will be a single sharp peak in the centre of the pole figure (13).

To provide a good signal to background ratio a relatively high loading of silicate is required. Hence a plate with 20% mica was used for these measurements. The diffraction pattern of this material showed a clear peak at 26.72°. This diffraction angle is equivalent to a spacing of 3.33Å, which is the lattice plane indexed *003* (14, 15). Hence the diffraction angle (2θ) was set to this value prior to performing scans through the range of tilt and rotation angles. As mica cleaves along *00l* planes then diffracting at this specific angle gives access to the orientation of the flakes. When the tilt and rotation angles are equal to zero then there is a perfect orientation of the flakes parallel to the surface of the plate.

The variation of the particle orientation with depth into the plate was investigated by analysing the surface of the plate, then machining down by a depth of 0.5 or 1mm before analysing the plate again.

It should be noted that the analysis volume depends upon the penetration depth of the X-rays, which varies with the value of 2θ used. As the value of 2θ is increased, so the depth of analysis will increase. However, the depth can be calculated using a standard X-ray penetration depth analysis (13) and the absorption coefficients of the elements (13). The number of X-rays which are absorbed by the sample, and hence which are not recorded, increases exponentially with depth. For the texture analysis a value of $2\theta=26.72°$ was used, and 90% of the signal comes from X-rays

which penetrated no further than about 100μm into the plate. Hence the analysis depth is small compared to the machining steps used.

The WAXS texture data from the surface of the plate are shown on a three-dimensional pole plot in Figure 2.1. The data show a large peak at the centre of the plot. The origin (centre) of these pole plots corresponds to a zero tilt and hence this corresponds to platelets that are orientated with the diffracted lattice plane *00l* parallel to the surface of the plate. The radial direction indicates deviation from this alignment. At the edge of the pole plot the lattice planes of the particles are perpendicular to the plate surface. A flat distribution of intensities in the radial direction would indicate a random distribution of particle orientation (13). Hence the peak at the centre of the pole plot in Figure 2.1 clearly shows that the particles at the surface of the plate are orientated parallel to the surface. This is expected as the plates are cast in a mould and hence the interaction of the particles in the liquid resin with the mould surfaces will tend to align the platelets parallel to the surface.

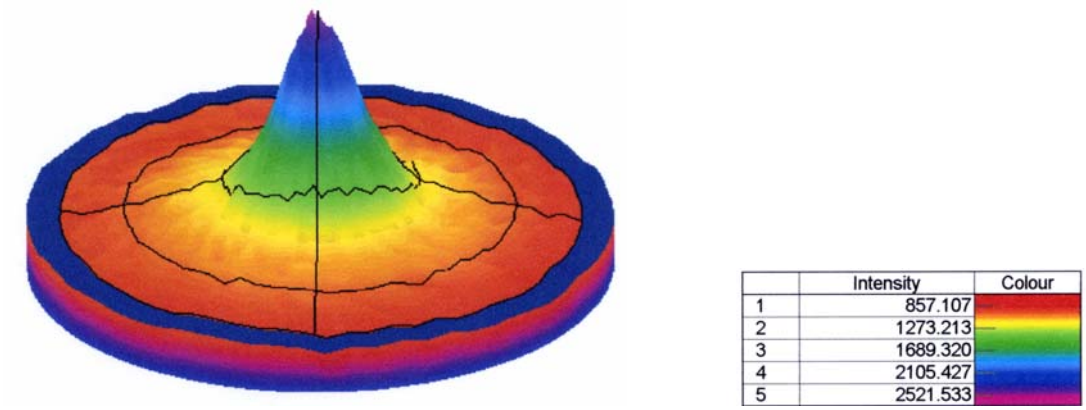

Figure 2.1: WAXS texture analysis data for epoxy with 20% mica, at surface of plate.

These data can also be displayed as a contour map, as shown in Figure 2.2a, on a two-dimensional pole plot. Here the contours are set at a constant relative intensity. Hence the sharp peak is represented by contours that are close together and close to the origin. Away from the surface of the plate there is less orientation, see Figures 2.2b-d, as the contours become further apart and the peak becomes less intense. Hence in the bulk of the plate the particles are not so highly orientated, but they do not show a random orientation, as the intensities are not constant across the whole plot. This may be expected as the plates are relatively thin, being 6mm in thickness, and hence an orientation effect would be anticipated even well away from the surface.

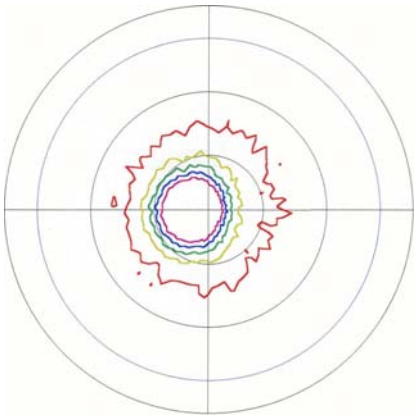

a) Surface

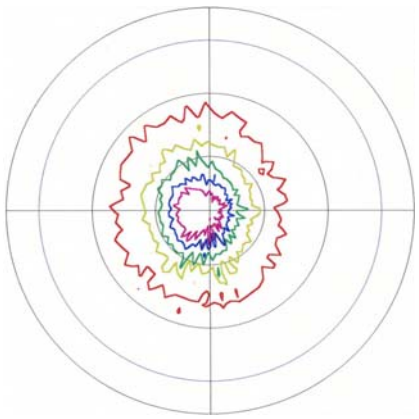

b) At 1mm depth

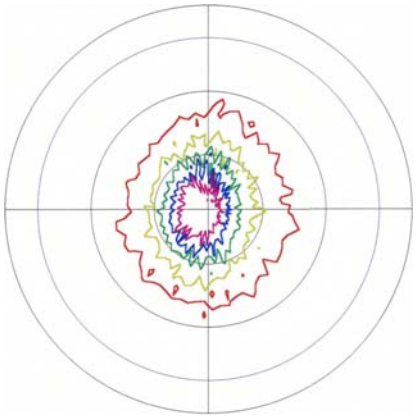

c) At 2mm depth.

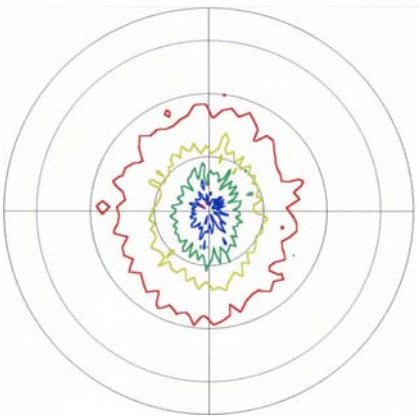

d) At 2.5mm depth.

	Intensity	Colour
1	1.000	
2	1.250	
3	1.500	
4	1.750	
5	2.000	

Figure 2.2: WAXS texture analysis data for epoxy with 20% mica: a: surface of plate, b: at 1mm depth, c: at 2mm depth, d: at 2.5mm depth, showing orientation of platelets at the surface of the plate and less orientation within the plate. (Contours shown at relative intensities of 1 to 2, with increments of 0.25.)

Note that the surface data exhibit a peak slightly decentred from the z-axis by 7.3°, see Figure 2.2a. This deviation is significant enough to indicate that the platelets at the surface are not exactly parallel to the surface, but are slightly tilted. This discrepancy is thought to result from the moulding process, as the plates are cast in a vertical mould. Hence there will be a small amount of sedimentation during curing, which leads to some tilting of the particles.

2.3.3 Effect of Specimen Orientation on Measured Fracture Toughness

A fracture toughness, K_c, value of 1.0MPam$^{1/2}$ was measured for the unmodified epoxy. This is a typical value for an unmodified thermosetting polymer in the glassy region (1). Modification with Cloisite 25A gives a significant toughening effect, a mean K_c value of 1.5MPam$^{1/2}$ being measured using 5% Cloisite 25A, as shown by the first bar in Figure 2.3. This value is in good agreement with previous work (16), and represents an increase of 50% compared with the toughness of the unmodified epoxy.

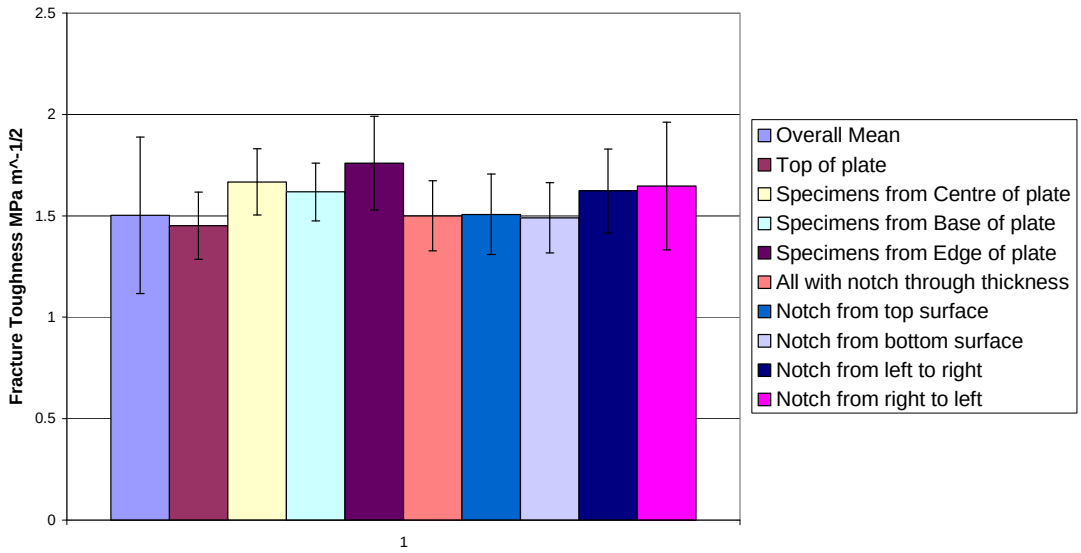

Figure 2.3: Fracture toughness values for different specimen positions and crack orientations, showing no effect of specimen orientation on measured fracture toughness, for epoxy with 5% Cloisite 25A.

The second to fourth bars of data in Figure 2.3 show the effect of taking the specimens from the top, centre or bottom of the plate. As the plate is cast in a vertical mould, then sedimentation might cause there to be differences in the fracture toughness. However, the standard deviations of the test data overlap, showing that there is no significant difference in the data – i.e. the values are identical within experimental error.

The effect of particle orientation can be seen by comparing the remaining columns of data with those already discussed. The specimens were machined such that all possible crack growth directions were tested. The data in Figure 2.3 show that the measured fracture energies are identical within experimental error, as the standard deviations of the test data overlap. Hence the observed orientation of the silicate particles has no effect on the fracture toughness.

2.4 Summary

Epoxy micro- and nano-composites have been manufactured using silicate modifiers, and the effect of the particle orientation that occurs during moulding has been investigated. The fracture toughness of the epoxy was increased by 50% with the addition of only 5% of Cloisite 25A. Wide angle X-ray scattering texture analysis was used to show the degree of orientation of the silicate particles. A significant orientation effect was observed, as the particles tended to align with the walls of the mould. However, the fracture toughness of specimens of epoxy with 5% of Cloisite 25A was unaffected by the particle orientation.

3 Fibre Composites with Nano-silica and Rubber Toughening

3.1 Introduction

The effect of the addition of nano-silica to fibre-composite materials has also been investigated, as this approach has the potential to increase the performance of these materials without significantly degrading the elevated-temperature performance. In addition, it is of interest whether the synergy between nano-silica and rubber noted in previous work (17) also exists with other epoxy formulations, and whether the increased toughness of the resin is transferred to an increase in toughness of the fibre composite.

The formulations used were based on diglycidylether of bisphenol A (DGEBA) with an anhydride curing agent (18). The formulations tested were an unmodified epoxy, nano-silica-modified, rubber-modified, and rubber & nano-silica modified epoxy. The rubber-modified epoxy formulation used 9% by mass of carboxyl-terminated butadiene (CTBN). The specimens were cured for 1 hour at 90°C plus 2 hours at 160°C.

3.2 Bulk Specimens

3.2.1 Introduction

Plates of bulk resin approximately 5mm thick were prepared by casting, and machined to produce tensile and fracture specimens.

3.2.2 Tensile Modulus

Tensile dumbbell specimens were machined from the plates of bulk resin and tested according to the relevant standards (19, 20, 21). Tests were conducted at room temperature and at a constant displacement rate of 1mm/min. A clip-on extensometer was used to measure the strain in the gauge length, and the Young's modulus was calculated.

The Young's modulus data are shown in Figure 3.1. The unmodified epoxy resin (0% rubber, 0% nano-silica) has a measured modulus of 3.0GPa, which agrees well with the expected value for a crosslinked epoxy polymer (1). The addition of nano-silica increases the measured modulus, and the addition of rubber lowers the modulus. This is as expected from particulate composite theory, as silica has a much higher modulus, and the rubber has a much lower modulus, than the epoxy. Overall, the modulus is relatively unchanged by the addition of nano-silica or rubber, the maximum value measured being 3.6GPa for the formulation with no rubber and 11% nano-silica.

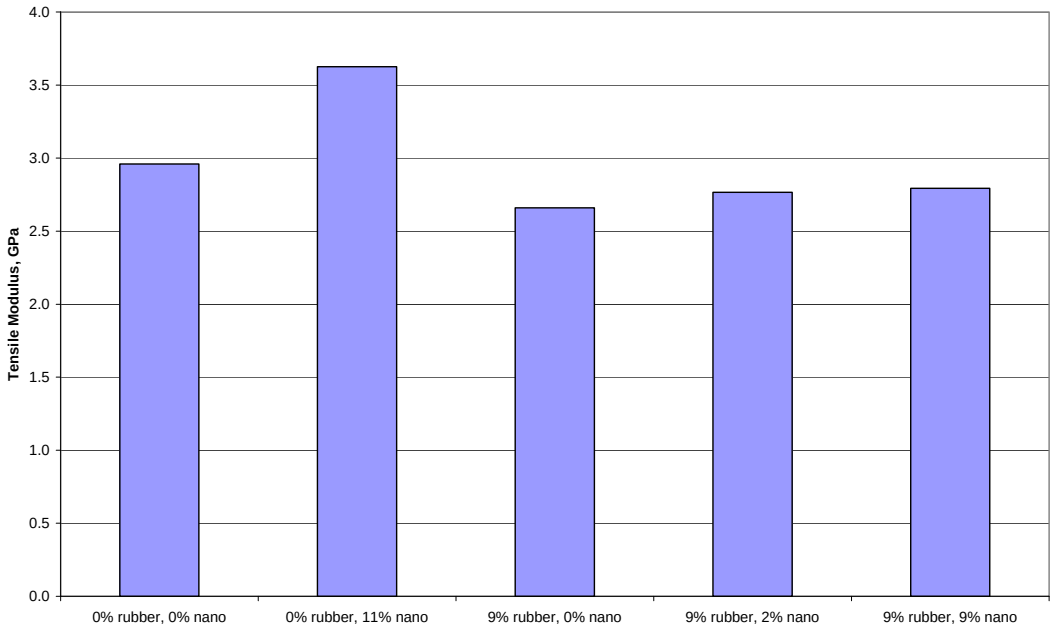

Figure 3.1: Modulus of bulk resin specimens.

3.2.3 Fracture Energy

The fracture toughness of the bulk resin was measured using single-edge-notch bend (SENB) tests, according to the relevant standards (12, 22). The tests were performed in three-point bending as described above at room temperature, using a constant displacement rate of 1mm/min. The maximum load was recorded, and the fracture toughness, K_c, was calculated. These values were converted to fracture energy, G_c, values using the standard analysis (12) and the measured values of modulus.

A fracture energy of 100J/m^2 was measured for the unmodified epoxy. This is a typical value for an unmodified thermosetting polymer in the glassy region (1). The addition of nano-silica increased the fracture energy, as shown in Figure 3.2. For example, the addition of 20% by mass of nano-silica gave a G_c of 630J/m^2, which is six times the unmodified resin value. Indeed, adding only 4% of nano-silica increased the fracture energy by over 200%, to 315J/m^2.

A rubber-modified epoxy formulation, with 9% by mass of carboxyl-terminated butadiene (CTBN), (i.e. 'hycar' from Noveon, USA) was also tested. This gave a fracture energy of 405J/m^2, an increase of 300% compared to the unmodified epoxy. The addition of nano-silica gave a further increase in the measured fracture energy, a maximum G_c of 1500J/m^2 being measured using 16% nano-silica (and 9% rubber). This value is an increase of 270% on the fracture energy of the rubber-modified (0% nano-silica) formulation, and of 1400% on the fracture energy of the unmodified epoxy. These data indicate that there is a synergy between the toughening effect of the rubber and the nano-silica, which leads to very large increases in the measured fracture energy.

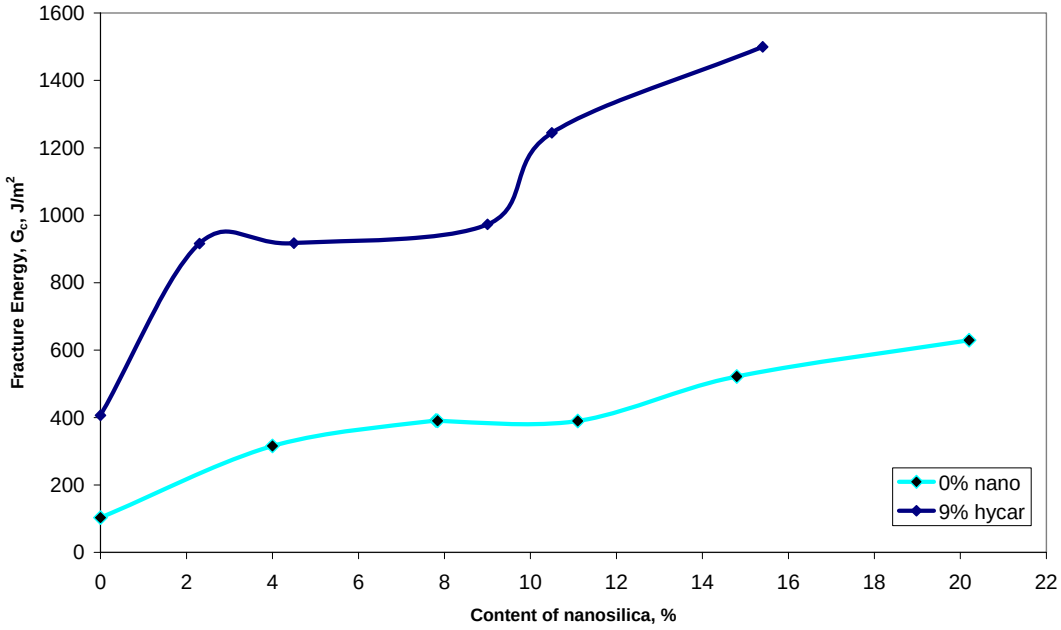

Figure 3.2: Fracture energy of bulk resin specimens versus nano-silica content.

3.3 Fibre Composites

3.3.1 Introduction

Plates of carbon fibre composite (CFRP), nominally 3mm thick, were manufactured by vacuum-assisted resin transfer moulding (VARTM). The same formulations as the bulk specimens discussed above were used. The fibre used was an isotropic woven carbon fibre fabric (98130, Interglas, Germany), with a density of 168g/m^2 and a linen weave. A thin film of PTFE was inserted into the fabric prior to resin infusion to act as a starter crack for the fracture specimens. The plates were machined to provide specimens for flexural and fracture testing.

3.3.2 Flexural Modulus

The flexural moduli of the CFRP specimens were measured according to the ASTM standard (23). Each plate was machined to give at least three specimens parallel to the starter crack, and three more in a perpendicular direction. This allowed the isotropy of the plates to be checked, i.e. whether the orientation of the specimens affected the modulus. All specimens were nominally 150mm long by 25mm wide. Four replicate tests were performed on each specimen, two on each face of the sample. The specimens were tested at a constant strain rate of 0.01/min in three-point loading, at 20°C. Load-displacement graphs were recorded, and the flexural modulus was calculated. Note that all the tests were elastic, and no permanent plastic deformation was observed.

The experimental data showed no particular trend, as shown in Figure 3.3. However, it was noted that the specimen thickness was not equal for each formulation, indicating that the fibre volume fraction would vary from one formulation to another. As the modulus of the composites is fibre-dominated, the actual volume fraction of fibres was measured using an acid dissolution process according to the relevant standard (24). It was found that the fibre volume fraction did indeed vary significantly. Hence the composite modulus was calculated using the measured moduli from the bulk resin tests and the measured fibre modulus, assuming a constant volume fraction of fibre. These data are shown in Figure 3.3, and indicate that the composite modulus is approximately constant. Hence, the addition of nano-silica and/or rubber has very little effect on the modulus of the composite. This is as expected, as the variations in the resin moduli are small, and the composite modulus is fibre-dominated.

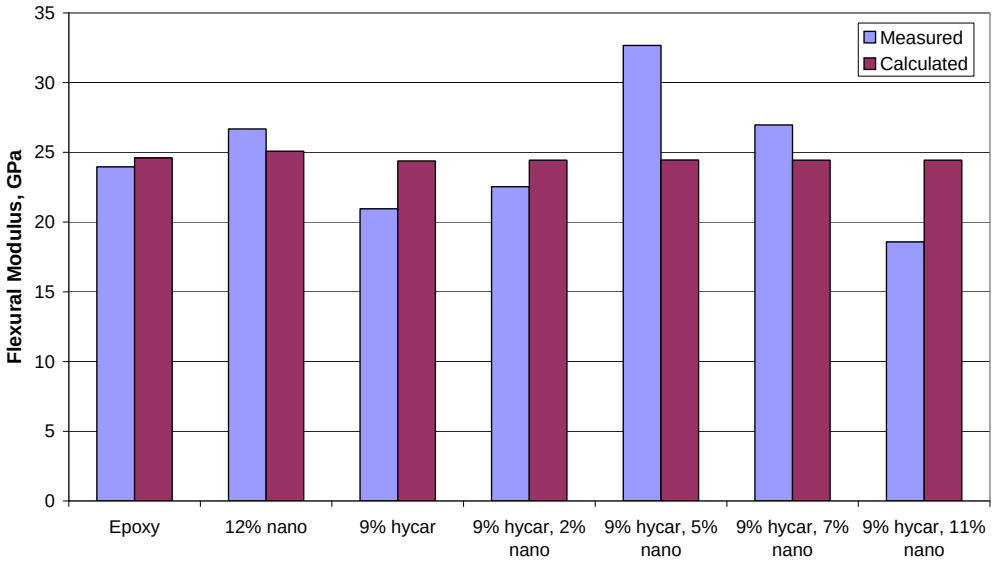

Figure 3.3: Flexural modulus versus content of nano-silica and rubber for carbon fibre laminates. (Measured moduli vary due to unequal fibre volume fractions, calculated moduli assume equal fibre volume fraction).

3.3.3 Double Cantilever Beam Specimens

Double cantilever beam (DCB) specimens were used to measure the fracture energy, G_c, of the CFRP plates. Specimens were cut from the CFRP plates with the pre-inserted starter crack at one end. Aluminium end-blocks were bonded onto either side of the sample. One side of each sample was painted white to allow the crack growth to be monitored during testing, and graduations were marked every 1mm. The specimens were tested in accordance with the ASTM standard (25). Specimens were tested at room temperature, at a test rate of 1mm/min. A travelling microscope was used to measure the crack length, and these data were recorded along with the load-displacement graphs. Each specimen was loaded in Mode I until crack growth was observed, and

then unloaded. After this precracking step, the specimen was loaded again, and the crack was grown for at least 80% of the length of the sample, and then unloaded. The crack length, load and displacement data were used to calculate the fracture energies, following the standard procedure (26).

The calculated fracture energies are shown in Figure 3.4. These data show that the CFRP with the unmodified matrix has a fracture energy, G_c, of 440J/m^2. The addition of 12% by mass of nano-silica increases G_c significantly, to 490J/m^2. The addition of 9% by mass of rubber causes a very large increase in the fracture energy, to 1040J/m^2, see Figure 3.4. Adding nano-silica to the rubber-modified epoxy matrix increases G_c further, a maximum value of 1320J/m^2 being measured using 11% nano-silica. This is an increase of 200% compared to the CFRP with the unmodified resin.

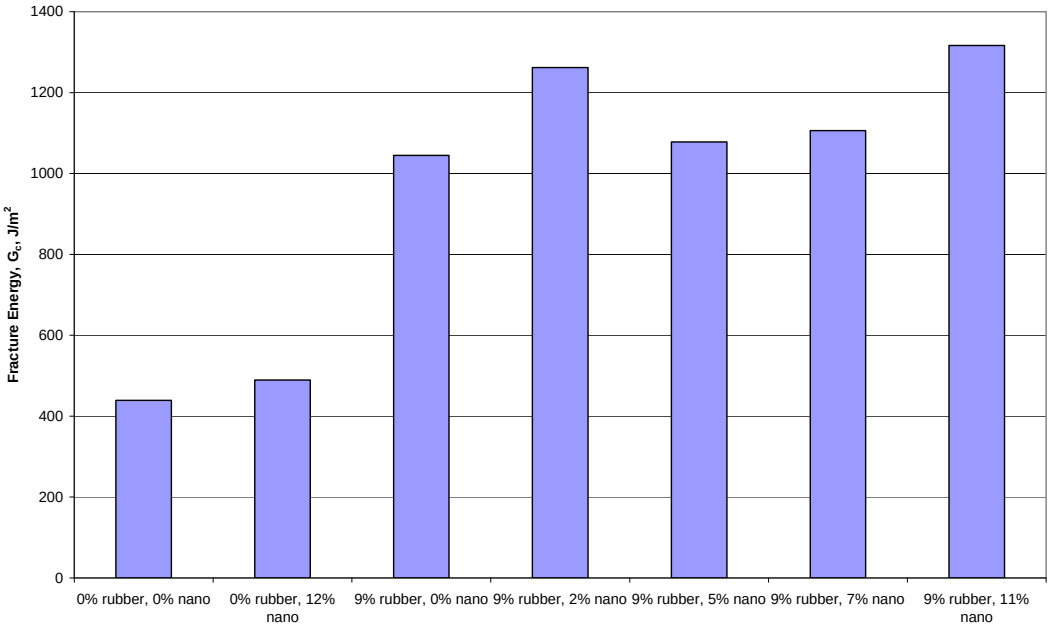

Figure 3.4: Fracture energies versus nano-silica content for carbon fibre laminates.

The measured fracture energies can be compared to those of the bulk resin, as shown in Figure 3.5. Note that the glass transition temperatures, T_g, of the bulk resin are also shown in this figure. The T_g values show that the addition of rubber reduces the glass transition temperature, but the addition of nano-silica has little effect on T_g. Figure 3.5 shows that there is a good correlation between the composite and the bulk fracture energies, but the composite values are generally higher due to the additional energy dissipation processes (e.g. fibre bridging) that occur in composite materials (27).

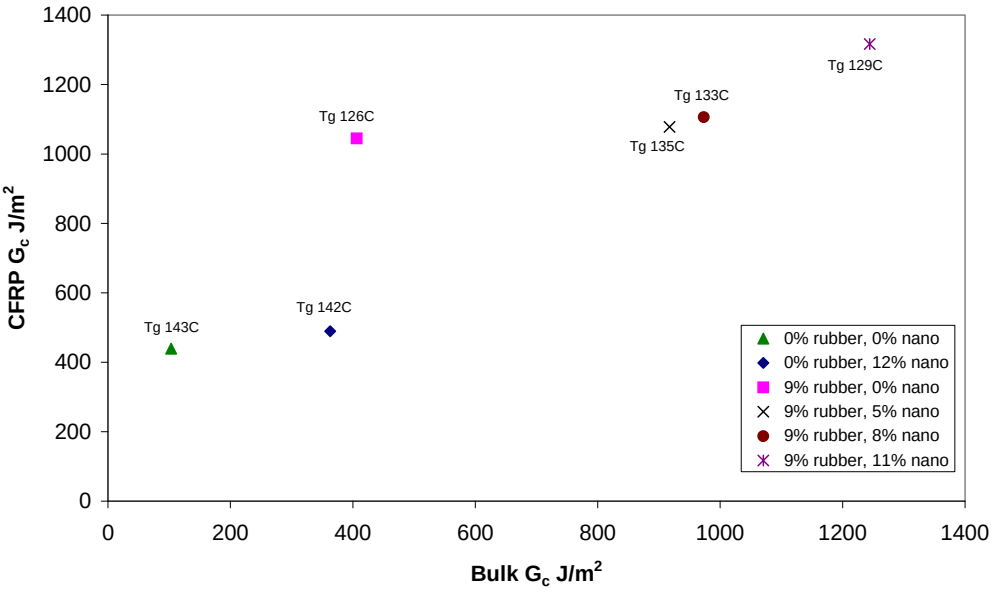

Figure 3.5: Fracture energy of CFRP laminates versus fracture energy of bulk resin, with glass transition temperatures.

3.4 Summary

The addition of nano-silica to epoxy resin significantly increased the measured fracture energy, G_c, when tested as bulk samples. The addition of rubber also gave an increased fracture energy. However, the addition of both rubber and nano-silica gave a further increase in the value of G_c. Indeed, the maximum value of the fracture energy measured was 1500J/m^2, which is 15 times that of the unmodified epoxy. Hence there is a significant synergy between the rubber and the nano-silica. Testing of CFRP using the same formulations also gave increased fracture energies, and showed that the high G_c values measured in the bulk were carried through to the composite toughness.

Finally it should be noted that the addition of the nano-silica, which is formed in-situ, at the levels employed in the present study give no significant increase in the viscosity of the resin system. This is an ideal situation for the VARTM, or a similar process.

4 Nanotube-Modified Epoxy Adhesives

4.1 Introduction

The toughening effect of carbon nanotubes was investigated using two different approaches, and fracture tests were performed on adhesive joint specimens in both cases. Firstly, nanotubes were added to a low-viscosity epoxy and aligned by the application of an electric field across the substrates. Three types of specimen were used, namely a control with no nanotubes, a random orientation of nanotubes, and nanotubes aligned by an electric field. Secondly, a preformed mat of aligned nanotubes was impregnated with a low-viscosity epoxy resin.

4.2 Alignment by Electric Field

4.2.1 Experimental

The double-cantilever beam (DCB) specimen geometry was used. Aluminium-alloy substrates, 6mm thick by 10mm wide and 125mm long, were used. Prior to bonding, the substrates were solvent cleaned in hot trichloroethylene, and etched in chromic-sulphuric acid for 20 minutes at 69°C (28). The substrates were rinsed with tap water, placed in a bath of tap water for 10 minutes, and rinsed with distilled water. The substrates were then dried in an oven at 60ºC for 30 minutes.

The epoxy used was a diglycidylether of bisphenol A (DGEBA) (LY556, Huntsman) cured with an amine hardener (XB3473, Huntsman). For the random and aligned specimens, multiwalled carbon nanotubes (MWNT) were added to the resin and mixed in thoroughly. The amine hardener was added, and the formulation was mixed again. This formulation was poured onto the substrates and spread using a spatula. A shim of PTFE was placed at either end of the substrates to control the thickness of the adhesive layer. Three adhesive layer thicknesses were used, namely 0.1, 0.5 and 1.0mm. A PTFE foil (10μm thick) was placed on each substrate, extending 20 mm from the loading point, to act as a starter crack. The joints were closed and clamped using foldback clips. For the electric field alignment, a crocodile clip was attached to each substrate, and an electric field of 6V/mm or 3V/mm was applied across the adhesive layer. The specimens were placed in a fan oven at 80°C, and cured for 4 hours. After this time the electric field was switched off, and the specimens were postcured for 4 hours at 160°C. The specimens produced are listed in Table 4.1.

Fracture testing of the DCB joints was performed according to the method described in the British standard (26). Aluminium-alloy end-blocks were bonded on using a room-temperature curing cyanoacrylate adhesive. One side of each specimen was spray-painted with a thin layer of white paint, and a paper scale, marked every 1 mm, was adhered to the side of the substrate above the adhesive layer. The specimens were loaded at a constant displacement rate of 0.1mm/min until a crack was seen to propagate from the starter foil, when they were unloaded. This precracking stage ensures that there is a sharp precrack present in the specimen prior to the actual test. The specimens were loaded again at 0.1 mm/min, and the crack propagation was followed using a

travelling microscope. Force, displacement and crack length data were recorded. These data were analysed to provide values of the fracture energy. Note that no plastic deformation of the substrate arms of the DCB specimens was observed.

Table 4.1: Specimens used.

Specimen code	Type	Nanotube loading	Electric Field Applied	Adhesive thickness, mm
UNT-01	Control	0	-	0.1
UNT-05	Control	0	-	0.5
UNT-10	Control	0	-	1.0
RNT-01	Random	0.1%	-	0.1
RNT-05	Random	0.1%	-	0.5
RNT-10	Random	0.1%	-	1.0
ANT-01	Aligned	0.1%	6V/mm	0.1
ANT-05	Aligned	0.1%	6V/mm	0.5
ANT-10	Aligned	0.1%	3V/mm	1.0

4.2.2 Results

The measured fracture energies, G_c, are shown in Figure 4.1. These data show that the value of G_c increases with the thickness of the adhesive layer. The fracture energy of the control (no nanotube) formulations varies from 140 to 200J/m^2, values which are typical of a highly crosslinked thermoset. The addition of 0.1% by mass of carbon nanotubes appears to increase the measured fracture energy. However, the standard deviations of the data overlap and hence any increase is probably not significant.

The absence of a significant increase in toughness is not surprising, as 0.1% is a very small loading compared to systems where significant toughening effects have been observed. For example, 40% by mass of modifier is typically used for thermoplastic-modified systems (29), and 10% by mass of mica has been shown to give the highest toughness for mica-modified formulations (3, 16). Hence future work will investigate the effect of increasing the loading of nanotubes, though it should be noted that at high loadings alignment cannot be achieved because the adhesive becomes too conductive (30).

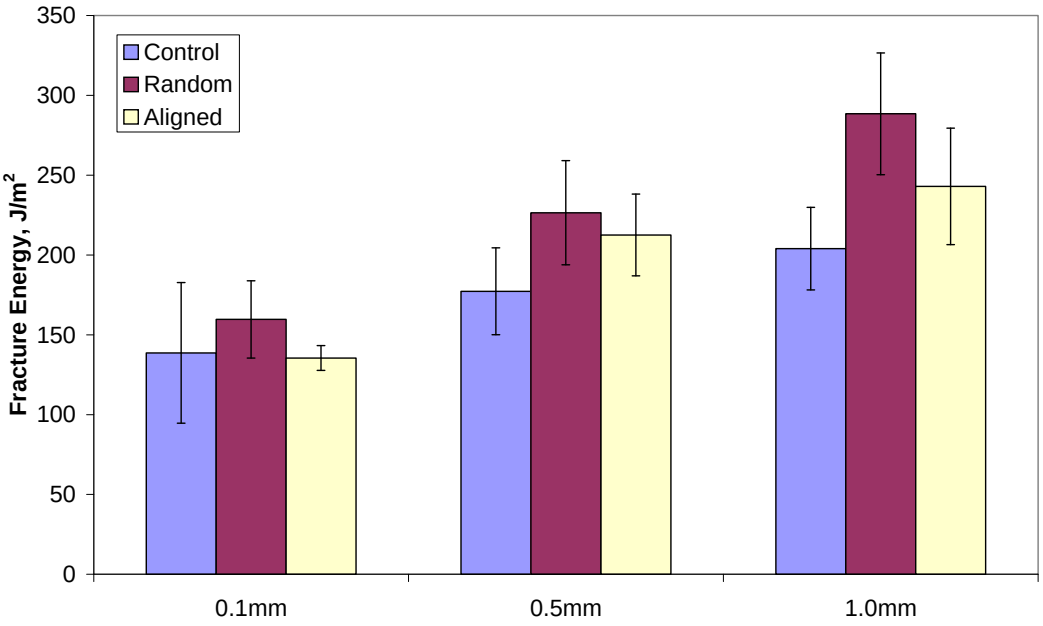

Figure 4.1: Fracture energy of epoxy (control), plus random- and aligned-nanotube modified epoxy, versus thickness of adhesive layer. Note that columns indicate the mean value, and error bars indicate the standard deviation

4.3 Impregnation of Nanotube Mats

4.3.1 Experimental

Carbon nanotube mats, grown on quartz substrates using chemical vapour deposition (CVD), were supplied by the University of Cambridge as part of an agreed joint programme. The quartz substrates were 100mm long by 10mm wide and 3mm thick, and the nanotubes were approximately 100μm long. A low-viscosity resin was formulated using a blend of epoxy resins and an anhydride curative, plus an advancement agent. The resin was poured onto the nanotube mat and allowed to flow between the nanotubes. Stainless steel wires with a diameter of 0.1 mm were placed at either end of the specimen to control the adhesive thickness, see Figure 4.2. A piece of PTFE film was placed at one end to act as a starter crack. A degreased quartz substrate was placed on top of the impregnated mat to form a DCB specimen. The specimens were cured for 1 hour at 120°C and 1 hour at 175°C, and then allowed to cool. Aluminium-alloy end-blocks were bonded on using a room-temperature curing cyanoacrylate adhesive. One side of each specimen was spray-painted with a thin layer of white paint, and a paper scale, marked every 1mm, was adhered to the side of the substrate above the adhesive layer. Fracture testing of the DCB joints was performed according to the method described in the British standard (26), as described above. Note that no plastic deformation of the substrate arms of the DCB specimens was observed.

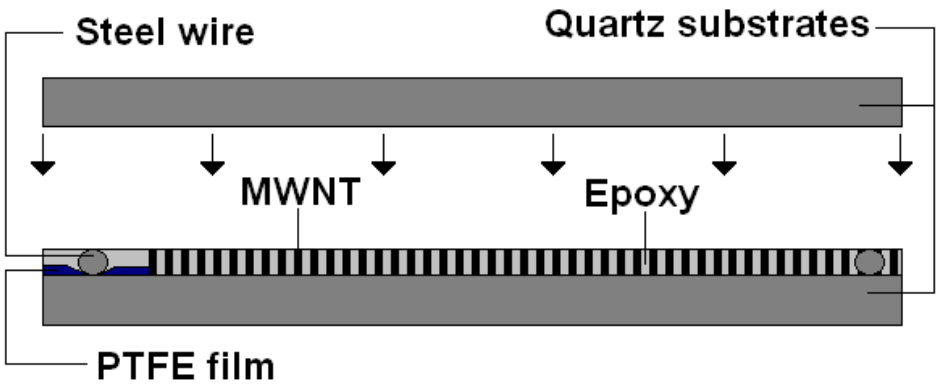

Figure 4.2: Schematic of the epoxy impregnated nanotube mat process.

4.3.2 Results

An example of the nanotube mat used is shown in Figure 4.3, sectioned parallel to the nanotube growth direction. This shows good alignment of the nanotubes, and the open nature of the mat should allow the epoxy to penetrate down to the substrate beneath.

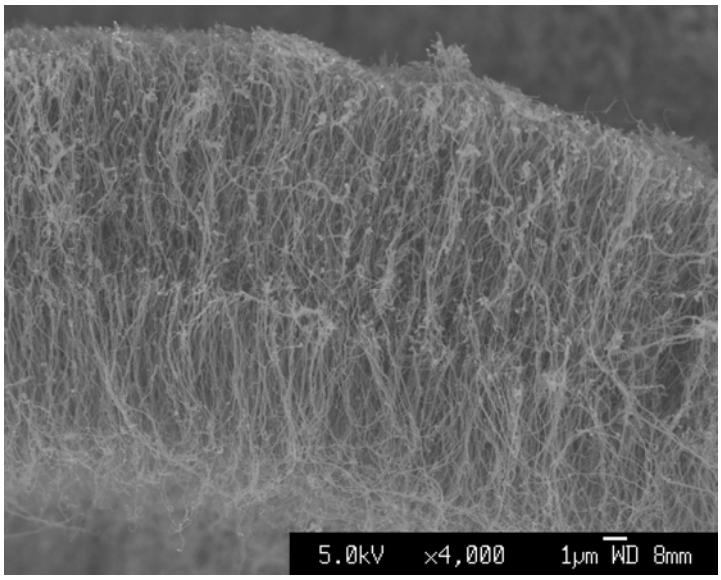

Figure 4.3: Carbon nanotube mat (31).

When tested, initially the impregnated mats exhibited poor adhesion to the quartz substrates. Hence for further tests the impregnated mat was transferred to aluminium-alloy substrates to improve the adhesion. This is a two-stage process, first one aluminium-alloy substrate is bonded on, then the quartz is removed and the second aluminium substrate is bonded on. However, fracture testing showed that the joints tend to fail at the interface between the impregnated mat and the adhesive on the second aluminium substrate.

Further tests using the quartz substrates showed that careful control of the impregnation process and the manufacture of the DCB specimens improved the adhesion between the impregnated mat and the substrates. However, though interfacial failures were eliminated, the quartz substrates failed by transverse or longitudinal splitting. To reduce the stresses on the quartz, aluminium-alloy backing beams were bonded on to stiffen the quartz substrates. However, failure still occurred in the quartz, and no values of the fracture energy could be measured. It appears that the residual stresses in the quartz substrates cause this premature failure, and hence future work will use silicon substrates.

In some cases, small areas of failure within the impregnated mat were observed. Scanning electron microscopy of the fracture surfaces of the epoxy impregnated carbon nanotube mat shows a high density of nanotubes, see Figure 4.4. The nanotubes are clearly visible, indicating that they may pull out of the epoxy matrix during crack propagation. This indicates that this impregnated mat technique has the potential to increase the fracture energy of the epoxy matrix.

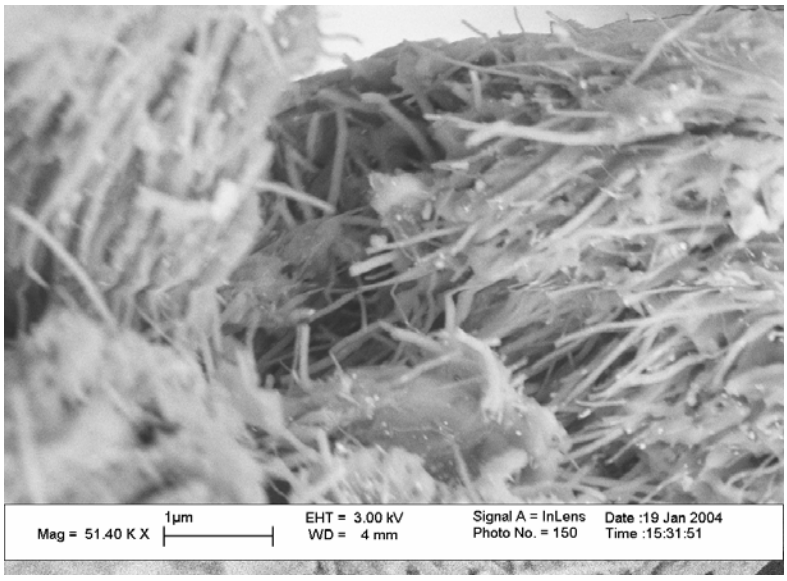

Figure 4.4: Scanning electron micrograph of epoxy impregnated carbon nanotube mat fracture surface.

4.4 Summary

The toughening effect of carbon nanotubes was investigated using two different approaches, and fracture tests were performed on adhesive joint specimens in both cases. Firstly, an electric field was used to align nanotubes in a low-viscosity epoxy. The field was applied during curing, prior to gelation of the epoxy. The measured fracture energies were compared to those from control formulations with no nanotubes, and to random orientations of nanotubes. The data showed that there was no significant effect of the addition of nanotubes, as the standard deviations of the data overlapped. However, the loading of nanotubes used was very low (0.1% by mass) and the data indicate that higher loadings may increase the toughness of the epoxy.

Secondly, a preformed mat of aligned nanotubes was impregnated with a low-viscosity epoxy resin. Successful impregnation of the epoxy into the mat was achieved using a specially-formulated low-viscosity resin. Problems were encountered due to fracture of the quartz substrates, and future work will use silicon substrates. However, some areas of failure within the impregnated mat were observed, which indicated that this impregnated mat technique has the potential to increase the fracture energy of the epoxy matrix.

5 Future Work

The work to date has shown how the mechanical and fracture properties vary with the microstructure of the epoxy composite (4, 5). The use of nano-modifiers can give significant increases in the mechanical and fracture properties of thermosetting epoxies. In addition, it has been demonstrated that the mechanical response of these materials can be predicted using finite-element modelling (6, 17).

There is, however, further work required to investigate some of the observed effects. In addition, the effect of particle orientation, the formation of multiphase materials, and modelling the performance of nanocomposites should be investigated.

The main aims of any future work should be:

- To produce polymer-matrix composites with a nano-phase of silica or carbon nano-tubes.
- To characterise the structure and mechanical properties of these composites, especially the fracture performance.
- To investigate the effect of orientation of the modifiers within the polymer matrix.
- To initiate and validate computational modelling studies to predict the performance of the composites.

6 Conclusions

Epoxy micro- and nano-composites have been manufactured using layered silicate modifiers, including mica and nanoclay, and the effect of the particle orientation that occurs during moulding has been investigated. Wide angle X-ray scattering texture analysis was used to show the degree of orientation of the silicate particles. A significant orientation effect was observed, as the particles tended to align with the walls of the mould. The fracture toughness of the epoxy was increased by 50% with the addition of only 5% of Cloisite 25A. However, fracture testing of specimens cut from orthogonal orientations showed that the fracture toughness was independent of specimen orientation. Hence, the orientation of the platelets has no effect on the fracture performance of silicate nano-composites.

The addition of nano-silica particles to the matrix of carbon fibre composites has been investigated. Both untoughened and rubber-toughened formulations were used, based upon an anhydride-cured epoxy. The addition of nano-silica leads to very significant increases in the toughness of the epoxy. The addition of nano-silica to epoxy resin significantly increased the measured fracture energy, G_c, when tested as bulk samples. The addition of rubbery particles also gave an increased fracture energy. However, the addition of both rubber and nano-silica gave a further increase in the value of G_c. Indeed, the maximum value of the fracture energy measured was 1500J/m^2, which is 15 times that of the unmodified epoxy. Hence there is a significant synergy between the rubber and the nano-silica particles. Testing of CFRP using the same formulations also gave increased fracture energies, and showed that the high G_c values measured in the bulk were carried through to the composite toughness. The nano-SiO_2 particles have an average particle diameter of 20 nm, and only a concentration of about 2% to 12% by mass of such nano-particles are needed to achieve significant improvements in the fracture performance; and it is especially noteworthy that the addition of the nano-silica, which is formed in-situ, at the levels employed in the present study give no significant increase in the viscosity of the resin system. This is, for example, an ideal situation for resin transfer, or infusion, moulding processes.

The toughening effect of carbon nanotubes and the effect of their orientation in adhesive joints has also been investigated, using two different approaches. Firstly, an electric field was used to align nanotubes in-situ in an adhesive joint by applying an electric field. The field was applied during curing, prior to gelation of the epoxy. The fracture energy of these aligned samples was measured and compared to control samples with no nanotubes, and to a random nanotube orientation. The measured fracture energies showed no significant effect of the addition and alignment of nanotubes. However, the loading of nanotubes used was very low (0.1% by mass) and the data indicate that higher loadings may increase the toughness of the epoxy.

Secondly, a preformed mat of aligned carbon nanotubes were grown on a quartz substrate, and impregnated with a low-viscosity epoxy resin. Successful impregnation of the epoxy into the mat was achieved using a specially-formulated low-viscosity resin. Problems were encountered due to premature failure of the quartz substrate, and hence current work is using silicon substrates. However, some areas of failure within the impregnated mat were observed, which indicated that this impregnated mat technique has the potential to increase the fracture energy of the epoxy matrix.

7 References

1. A. J. Kinloch, *Adhesion and Adhesives : Science and Technology* (Chapman & Hall, London, 1987).
2. A. J. Kinloch, *Proceedings of the Institution of Mechanical Engineers, Part G* **211**, 307-335 (1997).
3. A. J. Kinloch, A. C. Taylor, *Journal Of Materials Science* (To be published).
4. A. C. Taylor, A. J. Kinloch, A. E. Tarrant, Fracture and mechanical properties of epoxy modified with micro- and nanoparticles, J. T. Koberstein, G. L. Anderson, Eds., 26th Annual Meeting, Myrtle Beach, USA (The Adhesion Society, Blacksburg, USA, 2003).
5. A. J. Kinloch, A. C. Taylor, (To be published).
6. A. C. Taylor, H. Hadavinia, A. J. Kinloch, The Fracture and Mechanical Properties of Epoxy Micro- and Nanocomposites, Yield, Deformation & Fracture of Polymers, Cambridge (Institute of Materials, London, 2003).
7. A. Usuki, et al., *Journal of Materials Research* **8**, 1179-1184 (1993).
8. M. Alexandre, P. Dubois, *Materials Science and Engineering, R: Reports* **28**, 1-63 (2000).
9. R. A. Vaia, in *Polymer-Clay Nanocomposites* T. J. Pinnavaia, G. W. Beall, Eds. (John Wiley & Sons, Chichester, 2001) pp. 229-266.
10. R. A. Vaia, E. P. Giannelis, *Macromolecules* **30**, 8000 -8009 (1997).
11. X. Kornmann, H. Lindberg, L. A. Berglund, *Polymer* **42**, 4493-4499 (2001).
12. BS-ISO-13586, *Plastics - Determination of Fracture Toughness (GIC and KIC) - Linear Elastic Fracture Mechanics (LEFM) Approach* (BSI, London, 2000).
13. B. D. Cullity, *Elements of x-ray diffraction* (Addison-Wesley Publishing Company, Reading, MA, USA, ed. Second, 1978).
14. G. Brown, G. W. Brindley, in *Crystal structures of clay minerals and their X-ray identification* G. W. Brindley, G. Brown, Eds. (Mineralogical Society, London, 1980) pp. 305-359.
15. W. F. Bradley, R. E. Grim, in *The X-ray identification and crystal structures of clay minerals* G. Brown, Ed. (Mineralogical Society, London, 1961).
16. A. J. Kinloch, A. C. Taylor, *Journal Of Materials Science Letters* **22**, 1439-1441 (2003).
17. A. J. Kinloch, A. C. Taylor, "The effects of adhesion and nano-structure on the toughness of polymer nano-composites" *N62558-02-M-5603* (Imperial College London, 2003).
18. S. Sprenger, *Personal Communication* (Hanse Chemie, Geesthacht, Germany, 2004).
19. BS-2782:Part3, *Methods of Testing Plastics - Part 3 - Mechanical Properties. Method 322. Determination of Tensile Properties, Test Conditions for Moulding and Extrusion Plastics* (BSI, London, 1994).
20. ISO-527-2, *Plastics - Determination of tensile properties - Part 2: Test conditions for moulding and extrusion plastics* (ISO, Geneva, 1996).
21. ISO-527-1, *Plastics - Determination of tensile properties - Part 1: General principles* (ISO, Geneva, 1993).
22. ASTM-D5045, *Standard Test Method for Plane-Strain Fracture Toughness and Strain-Energy Release Rate of Plastic Materials*, ASTM (West Conshohocken, 1999).

23. ASTM-D790M, *Standard Test Method for Flexural Properties of Unreinforced and Reinforced Plastics and Electrical Insulating Materials (Metric)*, ASTM (West Conshohocken, 1993).
24. BS-EN-2564, *Carbon fibre laminates - Determination of the fibre, resin and void contents* (BSI, London, 1998).
25. ASTM-D5528, *Standard Test Method for Mode I Interlaminar Fracture Toughness of Unidirectional Fiber-Reinforced Polymer Matrix Composites* (ASTM, West Conshohocken, 1994).
26. BS-7991, *Determination of the mode I adhesive fracture energy, GIC, of structural adhesives using the double cantilever beam (DCB) and tapered double cantilever beam (TDCB) specimens* (BSI, London, 2001).
27. F. L. Matthews, R. D. Rawlings, *Composite materials : engineering and science* (Chapman & Hall, London, 1994).
28. *UK Defence Standard 03-2/2* (1983).
29. A. J. Kinloch, M. L. Yuen, S. D. Jenkins, *Journal of Materials Science* **29**, 3781-3790 (1994).
30. M. S. P. Shaffer, *Personal Communication* (Imperial College London, 2004).
31. I. A. Kinloch, *Personal Communication* (University of Cambridge, 2004).